

Fermilab Booster Dynamic Aperture Simulation with New Injection/Extraction Systems.

A. Drozhdin

Fermi National Accelerator Laboratory

P.O. Box 500, Batavia, Illinois 60510

July 14, 2005

1 Abstract

The results on Booster dynamic aperture simulation with new injection/extraction systems are presented.

2 Dynamic aperture simulation

The multiturn tracking of particles at dynamic aperture simulations in the Booster are done using STRUCT code [1]. The MAD program multipole coefficients of the order n with respect to the magnet center (also used in the STRUCT code) are presented in Tables 1 and 2. Magnetic field distributions in the FOCUSING and DEFOCUSING magnets are presented in Figs. 1 and 2. Beta functions, dispersion and beam orbit at injection calculated by STRUCT and MAD are shown in Fig. 3.

Horizontal and vertical phase plane for the Fermilab Booster with nonlinear fields in the injection and extraction systems and sextupole and octupole components in the main Foc and DeFoc magnets are shown in Figs. 4 and 5 for different horizontal and vertical betatron amplitudes. Phase planes for all nonlinear components in the main magnets are shown in Figs. 6 and 7. Information on the lost particles at this calculations are presented on the bottom of each figure.

Table 1: The MAD program multipole coefficients of the order n with respect to the magnet center $K_n \cdot L = 1/(B\rho) \cdot d^n BL/dx^n = 1/(3.3356405 \cdot 0.954263) \cdot d^n BL/dx^n [m^{-n}]$ for 0.4 GeV protons at new injection and extraction bump magnets. Input data to STRUCT code. Harmonics in a bump(max) are shown for maximum field in the magnet. Harmonics in a bump2a are shown for a case of bump2 rotated in the horizontal plane by 180° . Bump(max) and bump2 are not used in the system.

element	BL	$K_1 \cdot L$	$K_2 \cdot L$	$K_3 \cdot L$	$K_4 \cdot L$	$K_5 \cdot L$	$K_6 \cdot L$
	T-m	$1/m$	$1/m^2$	$1/m^3$	$1/m^4$	$1/m^5$	$1/m^6$
New injection bump magnets							
bump(max)	+1.5574E-01	+3.4188E-03	+9.9767E-03	+2.8903E+00	+2.2201E+02	-8.3869E+03	-3.6144E+06
bump1	-7.0028E-02	-1.5373E-03	-4.4860E-03	-1.2996E+00	-9.9829E+01	+3.7712E+03	+1.6252E+06
bump2	+1.4006E-01	+3.0745E-03	+8.9721E-03	+2.5993E+00	+1.9966E+02	-7.5424E+03	-3.2505E+06
bump2a	+1.4006E-01	-3.0745E-03	+8.9721E-03	-2.5993E+00	+1.9966E+02	7.5424E+03	-3.2505E+06
bump3	-7.0028E-02	-1.5373E-03	-4.4860E-03	-1.2996E+00	-9.9829E+01	+3.7712E+03	+1.6252E+06
New extraction bump magnets							
bump1	+7.5431E-02	-7.0906E-05	+4.5547E-02	+1.9956E-01	-8.1984E+00	-1.5063E+03	-3.5475E+05
bump2	-7.5431E-02	-7.8369E-05	+4.7016E-02	+1.3622E-01	-3.0061E+01	+1.2642E+03	+1.0748E+06
bump3	-7.5431E-02	+5.7844E-05	+4.8485E-02	+5.2060E-02	+8.1984E+00	-2.1518E+03	-5.6125E+05
bump4	+7.5431E-02	-9.3297E-07	+4.2608E-02	-5.3795E-02	+4.0992E+00	+1.4794E+04	-3.1769E+05

Table 2: Booster F and D-magnet field multipoles $b_n/B_o = (0.0254^n/n!B_o) \cdot d^n B/dx^n$ and STRUCT multipole coefficients $(L/B\rho) \cdot d^n B/dx^n$ at injection.

pole	n	F-magnet		D-magnet	
		$10^4 \cdot b_n/B_o$	$(L/B\rho) \cdot d^n B/dx^n$	$10^4 \cdot b_n/B_o$	$(L/B\rho) \cdot d^n B/dx^n$
			m/m^{n+1}		m/m^{n+1}
2	0	1.00000e+04	0.7793 kG	1.00000e+04	0.6627 kG
4	1	5.62210e+02	1.56589E-01	-7.02859e+02	-1.66472E-01
6	2	1.42220e+00	3.11902E-02	-3.91965e+00	-7.31000E-02
8	3	3.38836e-02	8.77677E-02	-2.98606e-01	-6.57743E-01
10	4	6.73212e-01	2.74614E+02	4.49709e-01	1.55997E+02
12	5	-4.33973e-01	-3.48474E+04	2.77620e-01	1.89571E+04
14	6	-1.08279e-00	-2.05385E+07	8.44590e-02	1.36233E+06
16	7	6.44508e-01	3.36913E+09	-2.13484e-01	-9.49002E+08
18	8	1.17022e-00	1.92670E+12	4.47200e-02	6.26124E+10
20	9	1.92633e-01	1.12379E+14	1.93170e-01	9.58312E+13
22	10	-8.00929e-01	-1.83956E+17	-1.16070e-02	-2.26701E+15
24	11	-2.47537e-00	-2.46218E+20	-1.73761e-01	-1.46975E+19

The results of these calculations are summarized in Fig. 8 where dynamic aperture of Booster is presented for the case with and without high order nonlinear components in the main magnets.

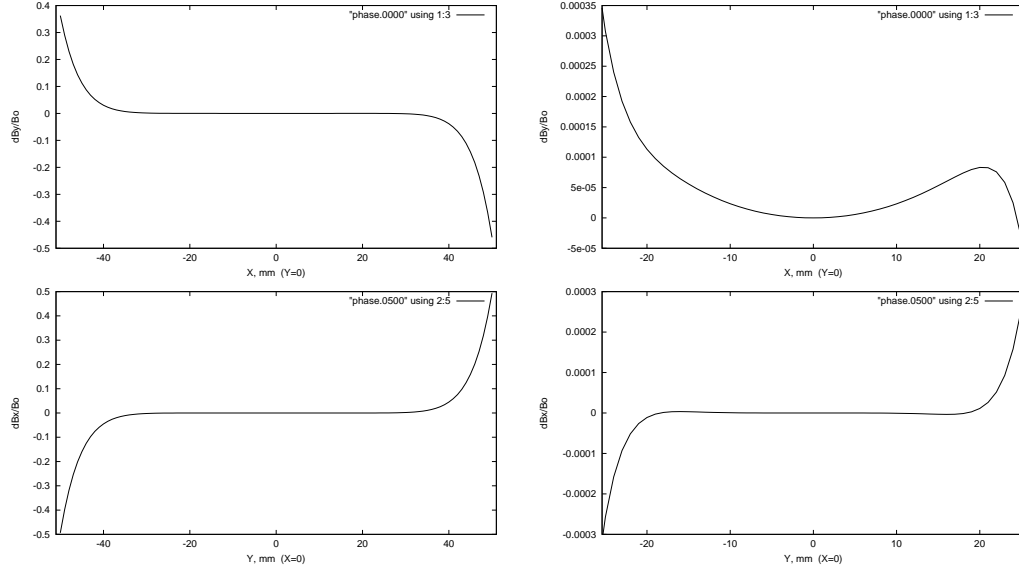


Figure 1: Magnetic field distribution in the FOCUSING magnet in a horizontal plane at $Y=0$ (top) and in a vertical plane at $X=0$ (bottom). Multipoles from $n=6$ to $n=24$ are taken into account. Right side - the same distributions in the range of $-25.4 \text{ mm} \leq X \leq +24.5 \text{ mm}$.

Horizontal and vertical phase plane of $\varepsilon_{95\%} = 7.8 \text{ mm} \cdot \text{mrad}$ (nominal emittance), $\varepsilon_{95\%} = 15.6 \text{ mm} \cdot \text{mrad}$ and $\varepsilon_{95\%} = 31.2 \text{ mm} \cdot \text{mrad}$ Gaussian distributed beam for Fermilab Booster with nonlinear components in the injection and extraction systems and all nonlinear components in the main Foc and DeFoc magnets are shown in Figs. 9 and 10 for the case without aperture restrictions and with real aperture of accelerator. There is no particle loss in the cases of $\varepsilon_{95\%} = 7.8 \text{ mm} \cdot \text{mrad}$ and $\varepsilon_{95\%} = 15.6 \text{ mm} \cdot \text{mrad}$ beams in both cases. About 20% of the beam is lost in a machine with real aperture for $\varepsilon_{95\%} = 31.2 \text{ mm} \cdot \text{mrad}$ beam.

3 Third order resonance correction

The normal sextupole components of injection, extraction system elements and main Booster magnets excite four types of resonances: $Q_x = 7$, $3Q_x = 20$, $2Q_y - Q_x = 7$ and $2Q_y + Q_x = 20$.

The skew sextupole components of injection, extraction system elements and

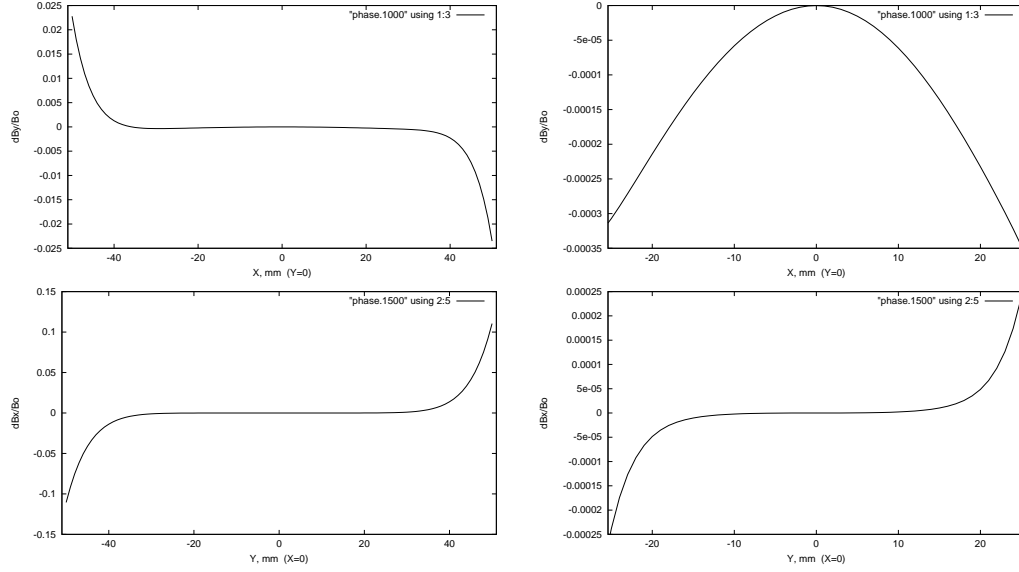


Figure 2: Magnetic field distribution in the DEFOCUSING magnet in a horizontal plane at $Y=0$ (top) and in a vertical plane at $X=0$ (bottom). Multipoles from $n=6$ to $n=24$ are taken into account. Right side - the same distributions in the range of $-25.4 \text{ mm} \leq X \leq +24.5 \text{ mm}$.

main Booster magnets excite other four types of resonances: $Q_y = 7$, $3Q_y = 20$, $2Q_x - Q_y = 7$ and $2Q_x + Q_y = 20$ (Fig. 11).

Correction of resonance $3Q_x = 20$ is performed by using normal sextupole correctors (Fig. 12) located at short straight sections of accelerator. As shown in the equations below the correctors located at short straight sections are a factor of $\beta_{x,short}^{3/2}/\beta_{x,long}^{3/2} = 13$ more efficient compared to correctors located at the long straight sections.

$$\Sigma A3_{reson} \beta_x^{3/2} \cos(3\psi_{x,reson}) = \Sigma S3_{corr} \beta_x^{3/2} \cos(3\psi_{x,corr})$$

$$\Sigma A3_{reson} \beta_x^{3/2} \sin(3\psi_{x,reson}) = \Sigma S3_{corr} \beta_x^{3/2} \sin(3\psi_{x,corr})$$

Here $A3_{reson}$, β_x , $\psi_{x,reson}$ are strength, β_x and phase of sextupole harmonic excited resonance;

$S3_{corr}$, β_x , $\psi_{x,corr}$ are strength, β_x and phase of sextupole harmonic used for correction.

Correction of resonance $2Q_y + Q_x = 20$ can be performed by using normal sextupole correctors located at short or long straight sections of accelerator. As shown in the equation below the correctors located at short straight sections are a

factor of $\beta_{x,long}^{1/2}\beta_{y,long}/\beta_{x,short}^{1/2}\beta_{y,short} = 2.3$ less efficient compared to correctors located at the long straight sections.

$$\begin{aligned}\Sigma A_{12_{reson}}\beta_x^{1/2}\beta_y\cos(2\psi_{y,reson} + \psi_{x,reson}) &= \Sigma S_{3_{corr}}\beta_x^{1/2}\beta_y\cos(2\psi_{y,corr} + \psi_{x,corr}) \\ \Sigma A_{12_{reson}}\beta_x^{1/2}\beta_y\sin(2\psi_{y,reson} + \psi_{x,reson}) &= \Sigma S_{3_{corr}}\beta_x^{1/2}\beta_y\sin(2\psi_{y,corr} + \psi_{x,corr})\end{aligned}$$

To check the performance of a new proposed correction scheme, the resonance $3Q_x = 20$ was excited by increasing of sextupole component of the main focusing magnet FMAGU01 by a factor of 10. Horizontal phase plane for $A_x = 0.5 - 4.0\sigma_x$ particles ($\varepsilon_{95\%} = 7.8 \text{ mm} \cdot \text{mrad}$) is shown in Fig. 13. All sextupole correctors of short straight sections are selected in four circuits: SIN+, SIN-, COS+, COS-. 16 correctors have a good phase directed close to direction of SIN+, SIN-, COS+, COS- vectors shown in Fig. 12. These correctors are called “main” correctors. Eight other correctors are directed at about 45° with respect to the SIN+, SIN-, COS+, COS- vectors. These correctors are called “additional” correctors. Using of these correctors may decrease the required corrector strength by 16%, as shown in Fig. 13. The existing now third order resonance correction scheme consists of only four correctors. As seen from Fig. 13, the new proposed correction system do not produce perturbation of phase ellipses (do not increase betatron amplitude) because correctors are uniformly distributed around the accelerator and do not produce big kicks to the particles compared to existing scheme. The maximum required strength of one corrector in the existing scheme is a factor of 50 higher compared to the new one, but the number of correctors is only a factor of 6 bigger.

References

- [1] I. S. Baishev, A. I. Drozhdin and N. V. Mokhov, “STRUCT Program User’s Reference Manual”, SSCL-MAN-0034 (1994); <http://www-ap.fnl.gov/~drozhdin/>.

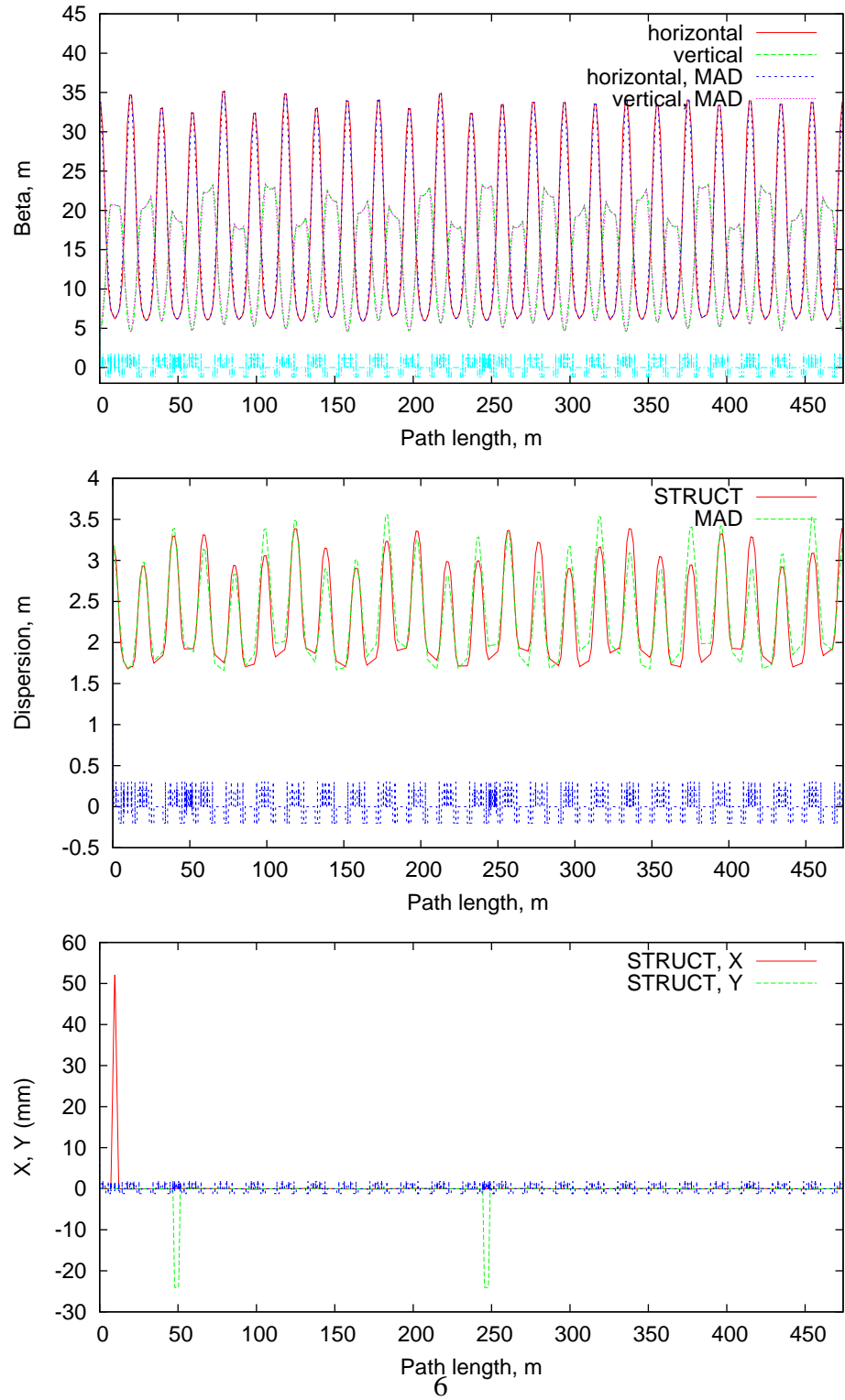


Figure 3: Beta functions, dispersion and beam orbit at injection calculated by STRUCT and MAD.

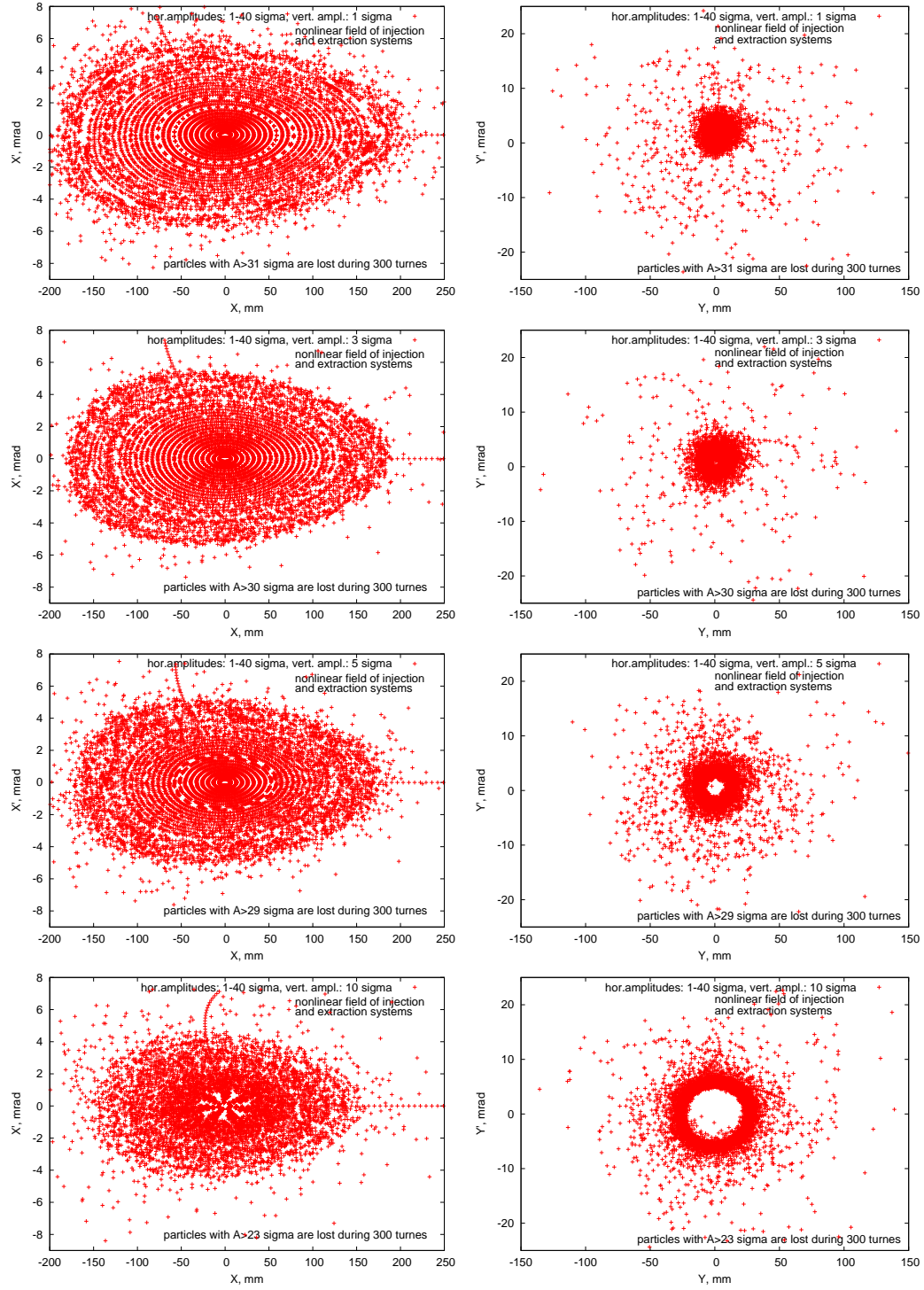


Figure 4: Horizontal (left) and vertical (right) phase plane for the Fermilab Booster with nonlinear fields in the injection and extraction systems. Only sextupole and octupole components are taken in the main Foc and DeFoc magnets.

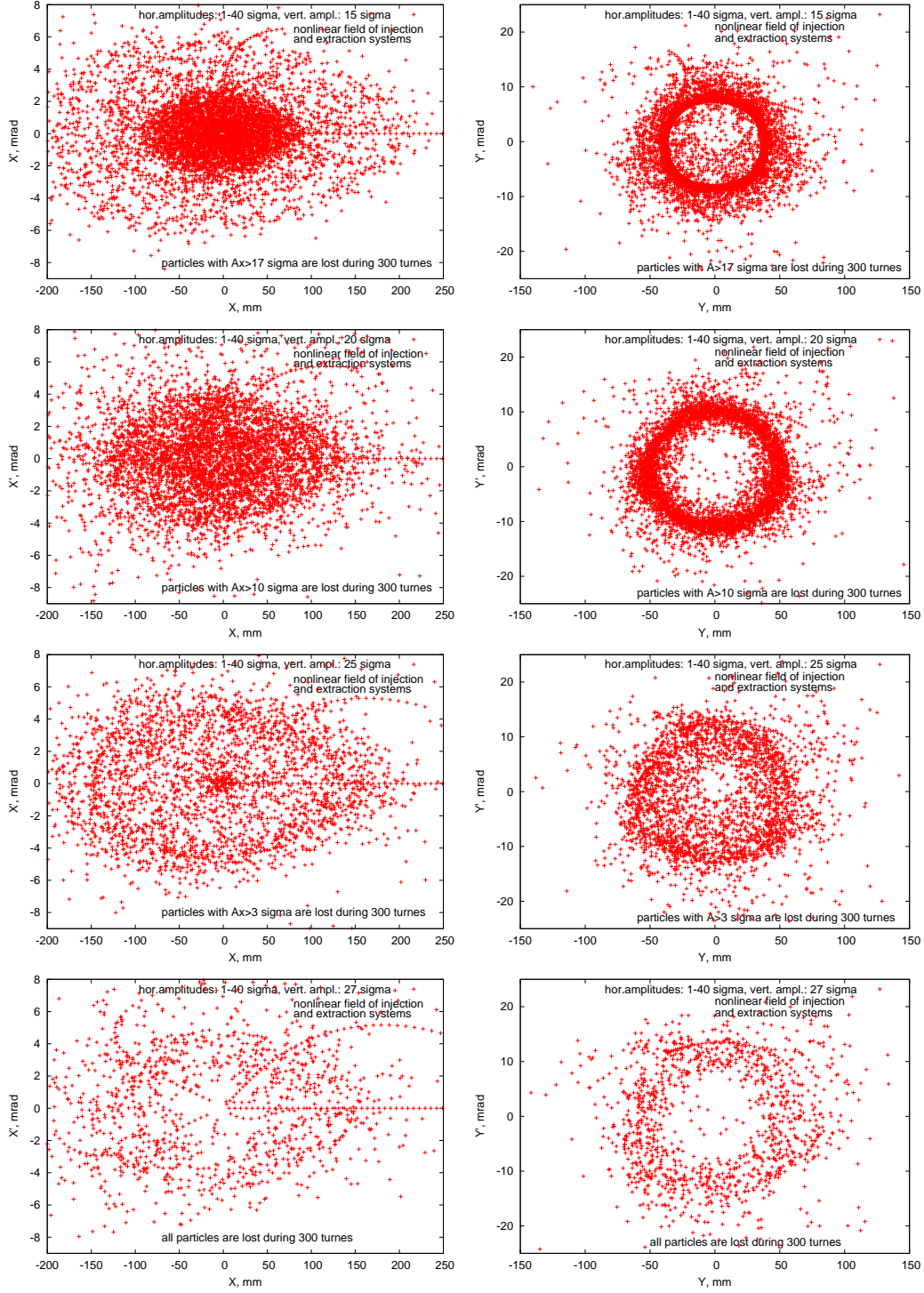


Figure 5: Horizontal (left) and vertical (right) phase plane for the Fermilab Booster with nonlinear fields in the injection and extraction systems. Only sextupole and octupole components are taken in the main Foc and DeFoc magnets.

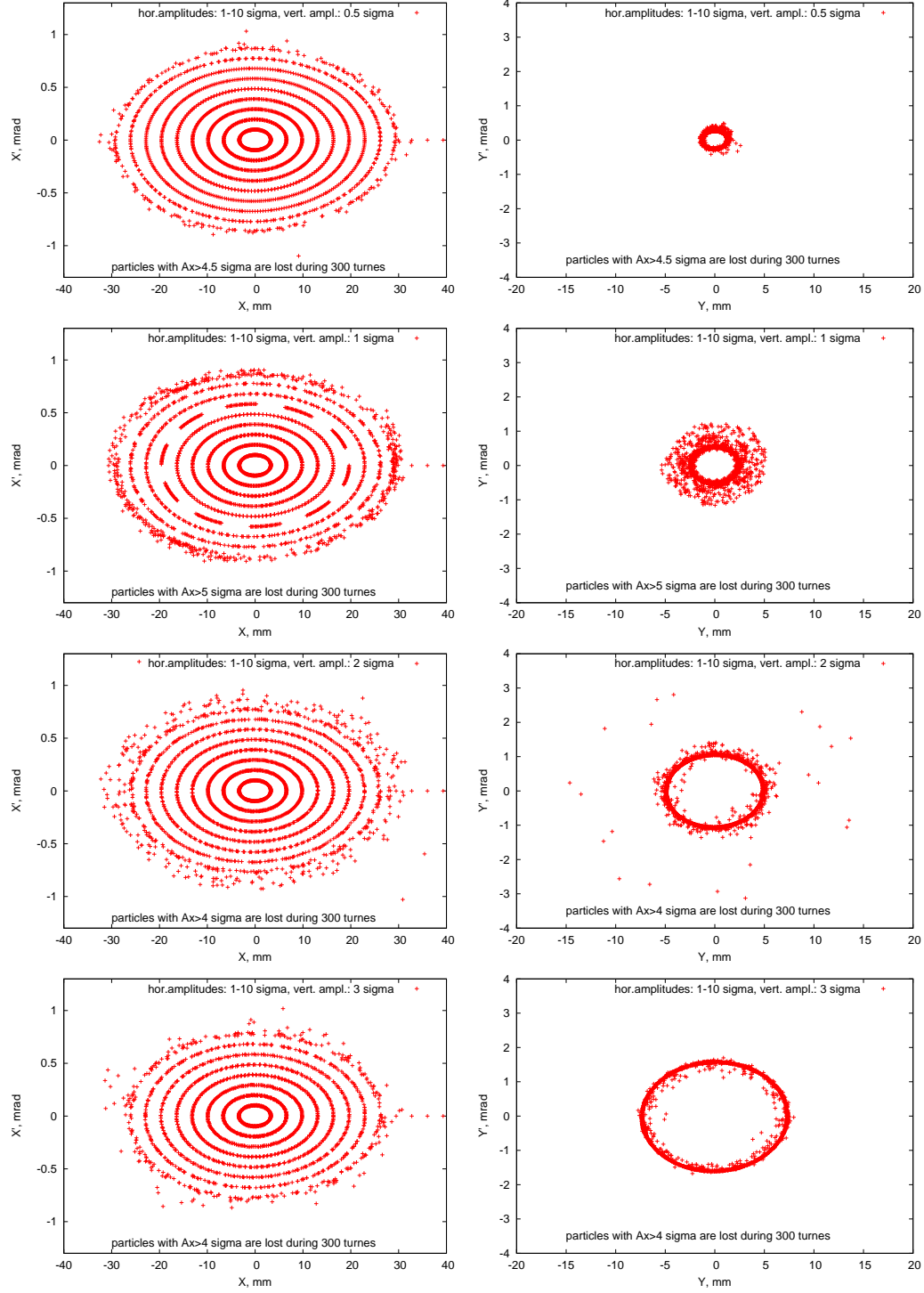


Figure 6: Horizontal (left) and vertical (right) phase plane for the Fermilab Booster with nonlinear fields in the injection and extraction systems. All nonlinear components are taken in the main Foc and DeFoc magnets.

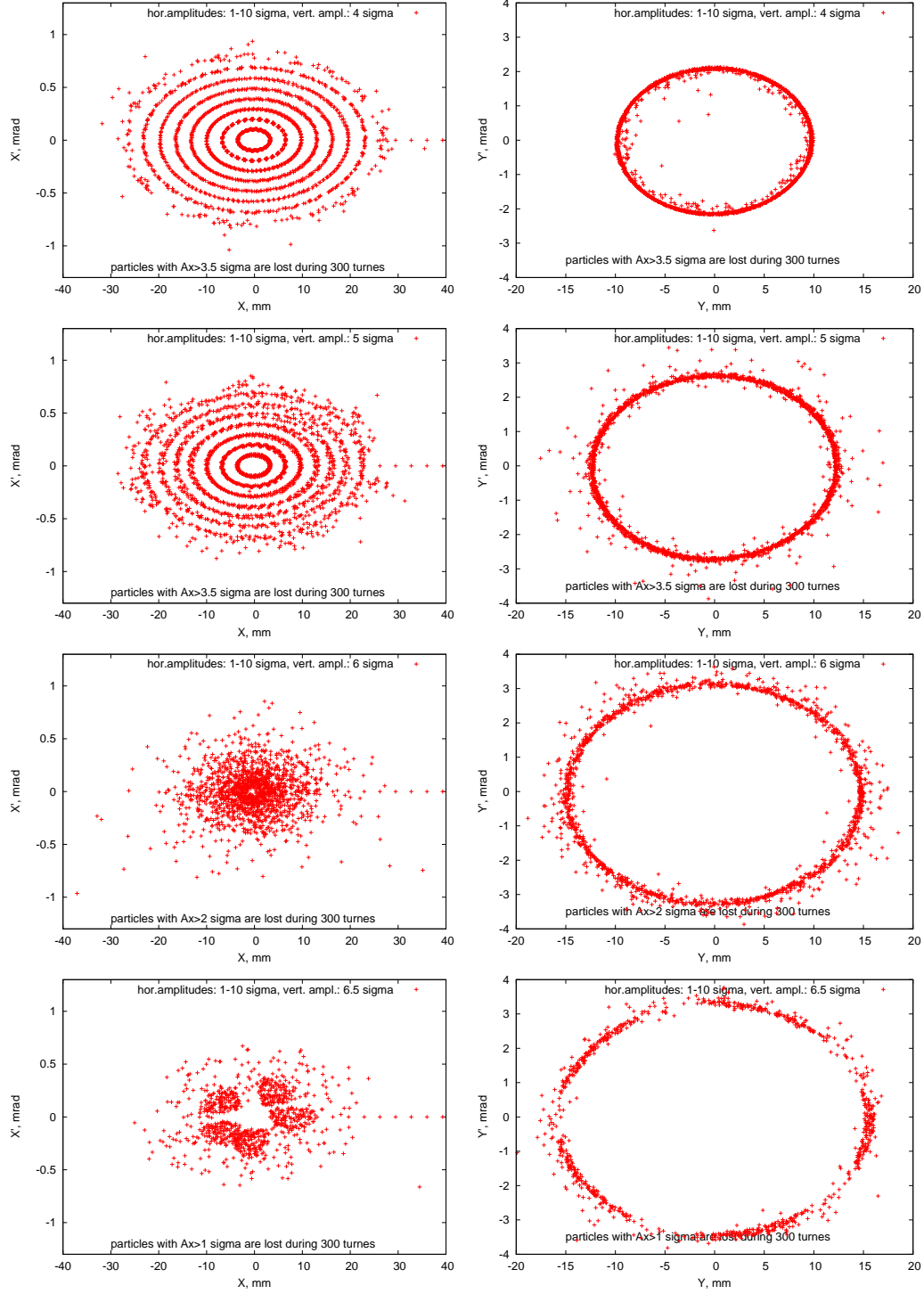


Figure 7: Horizontal (left) and vertical (right) phase plane for the Fermilab Booster with nonlinear fields in the injection and extraction systems. All nonlinear components are taken in the main Foc and DeFoc magnets.

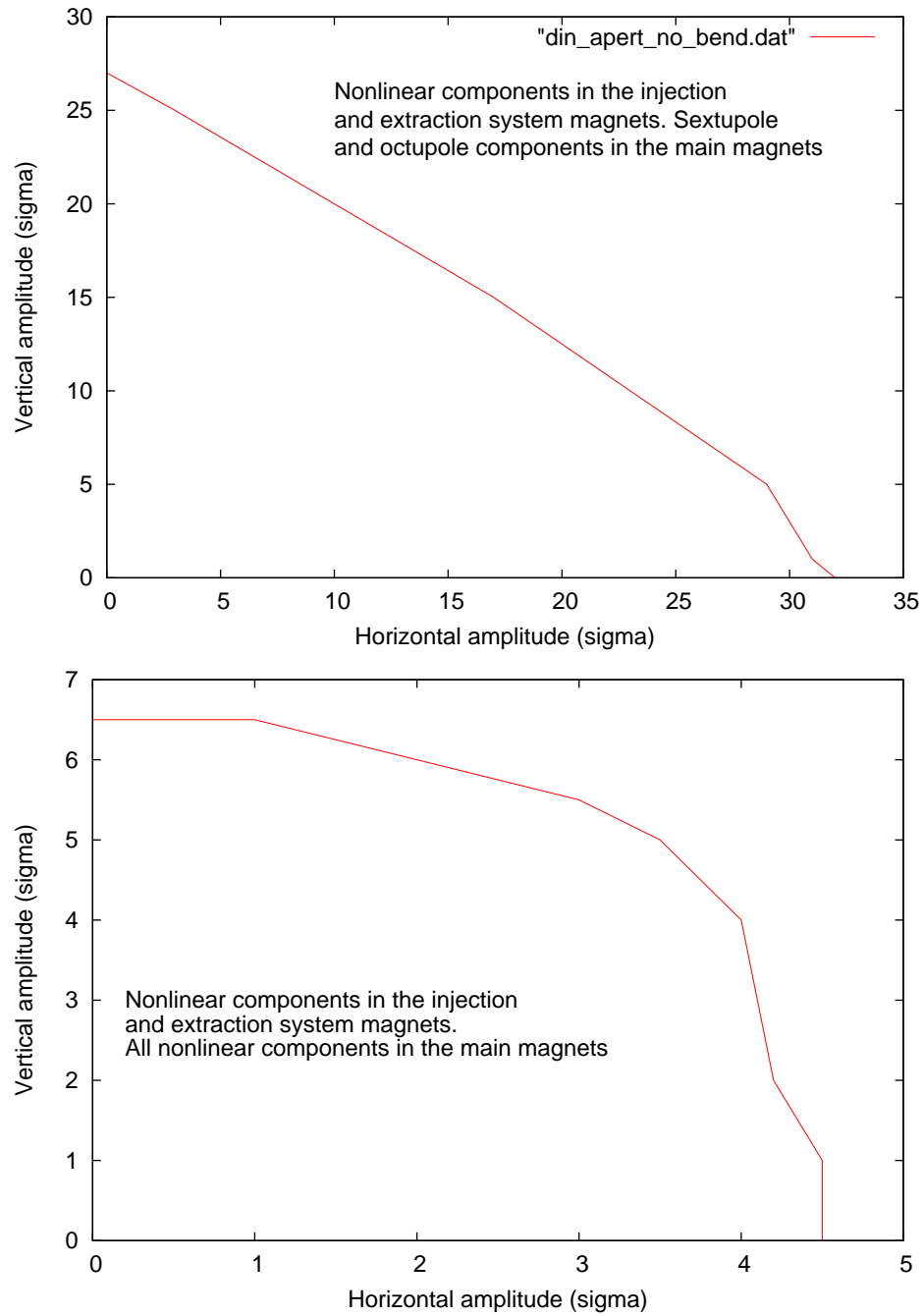


Figure 8: Dynamic aperture of Fermilab Booster with nonlinear components in the injection and extraction systems and sextupole and octupole components in the main Foc and DeFoc magnets (top). Dynamic aperture with all nonlinear components in the main magnets (bottom).

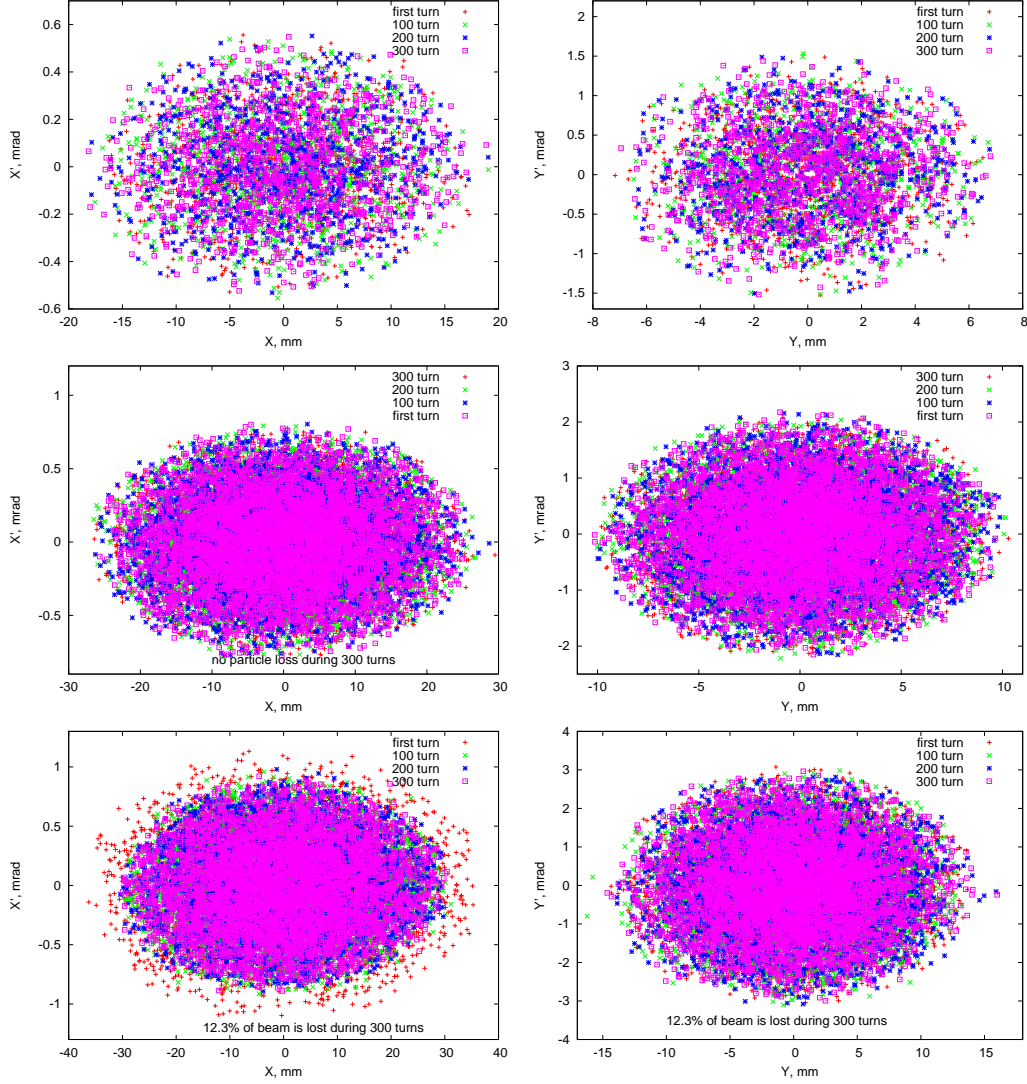


Figure 9: Horizontal (left) and vertical (right) phase plane of $\varepsilon_{95\%} = 7.8 \text{ mm} \cdot \text{mrad}$ (top), $\varepsilon_{95\%} = 15.6 \text{ mm} \cdot \text{mrad}$ (middle) and $\varepsilon_{95\%} = 31.2 \text{ mm} \cdot \text{mrad}$ (bottom) Gaussian distributed beam for Fermilab Booster with nonlinear components in the injection and extraction systems and all nonlinear components in the main Foc and DeFoc magnets. There is no aperture restriction in the accelerator (aperture in calculations is $R=420 \text{ mm}$). There is no particle loss in the cases of $\varepsilon_{95\%} = 7.8 \text{ mm} \cdot \text{mrad}$ and $\varepsilon_{95\%} = 15.6 \text{ mm} \cdot \text{mrad}$ beams. 12.3% of the beam is lost in the case of $\varepsilon_{95\%} = 31.2 \text{ mm} \cdot \text{mrad}$ beam.

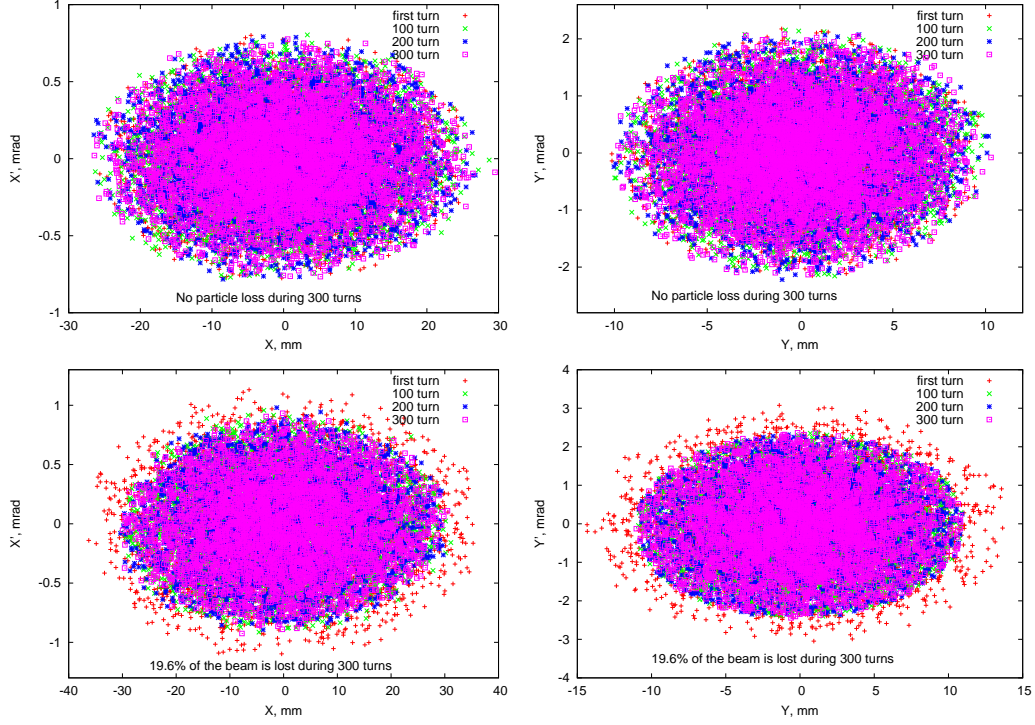


Figure 10: Horizontal (left) and vertical (right) phase plane of $\varepsilon_{95\%} = 15.6 \text{ mm} \cdot \text{mrad}$ (top) and $\varepsilon_{95\%} = 31.2 \text{ mm} \cdot \text{mrad}$ (bottom) Gaussian distributed beam for Fermilab Booster with nonlinear components in the injection and extraction systems and all nonlinear components in the main Foc and DeFoc magnets. Real aperture restrictions in the accelerator. There is no particle loss in the cases of $\varepsilon_{95\%} = 15.6 \text{ mm} \cdot \text{mrad}$ beams. 19.6% of the beam is lost in the case of $\varepsilon_{95\%} = 31.2 \text{ mm} \cdot \text{mrad}$ beam.

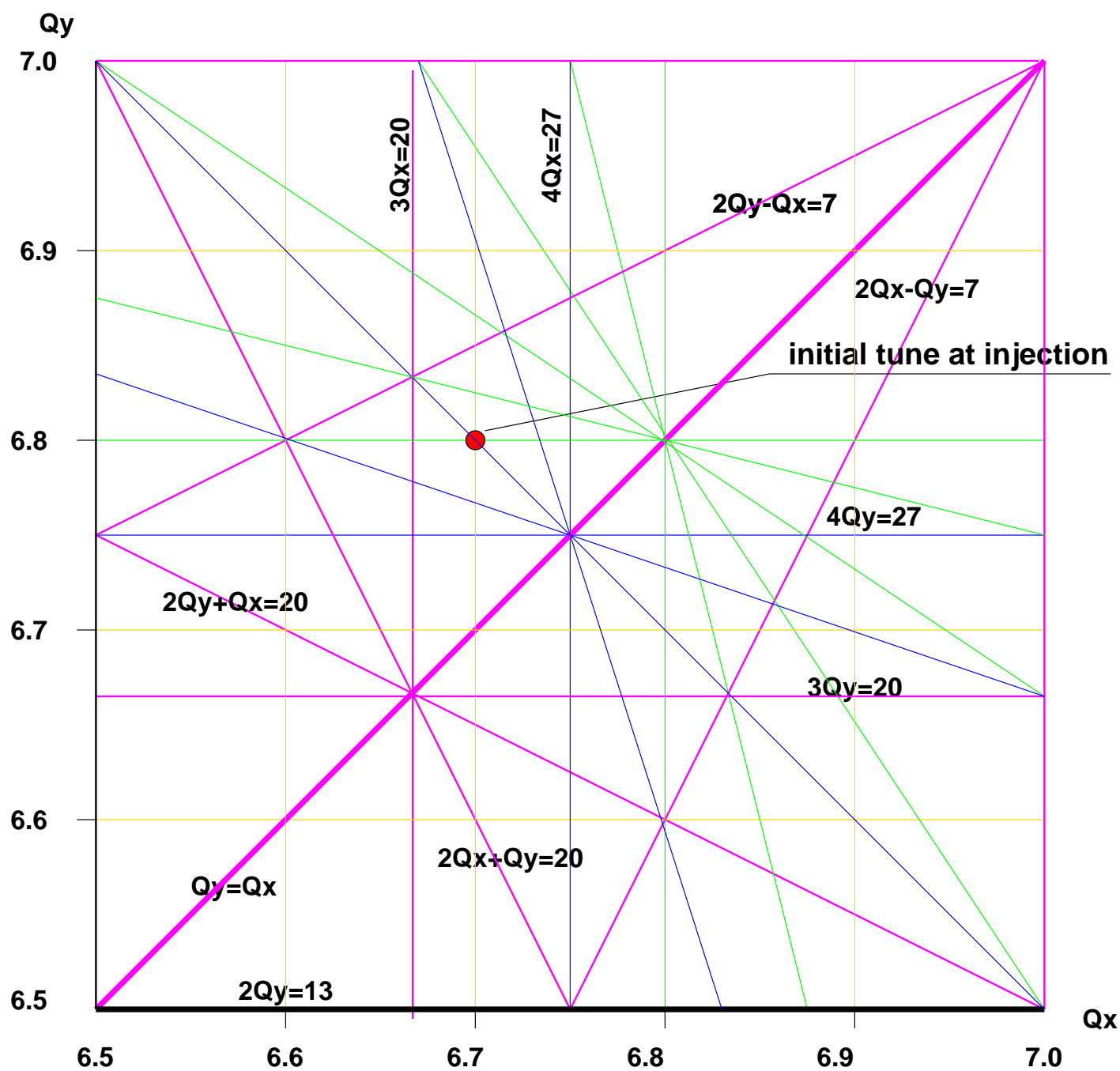


Figure 11: Booster tune plane.

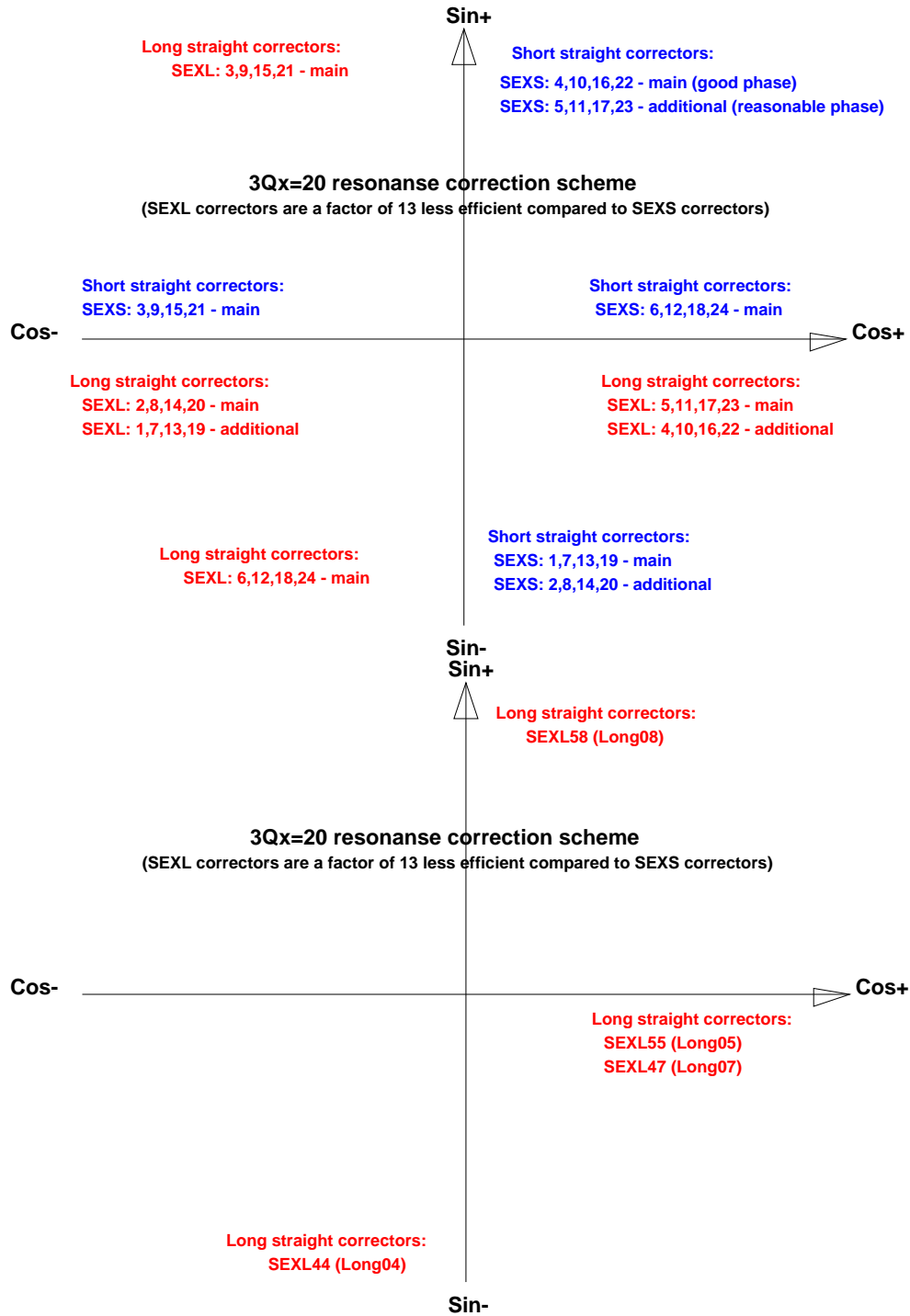


Figure 12: Third order resonance correction scheme. New correction system (top) and existing scheme (bottom).

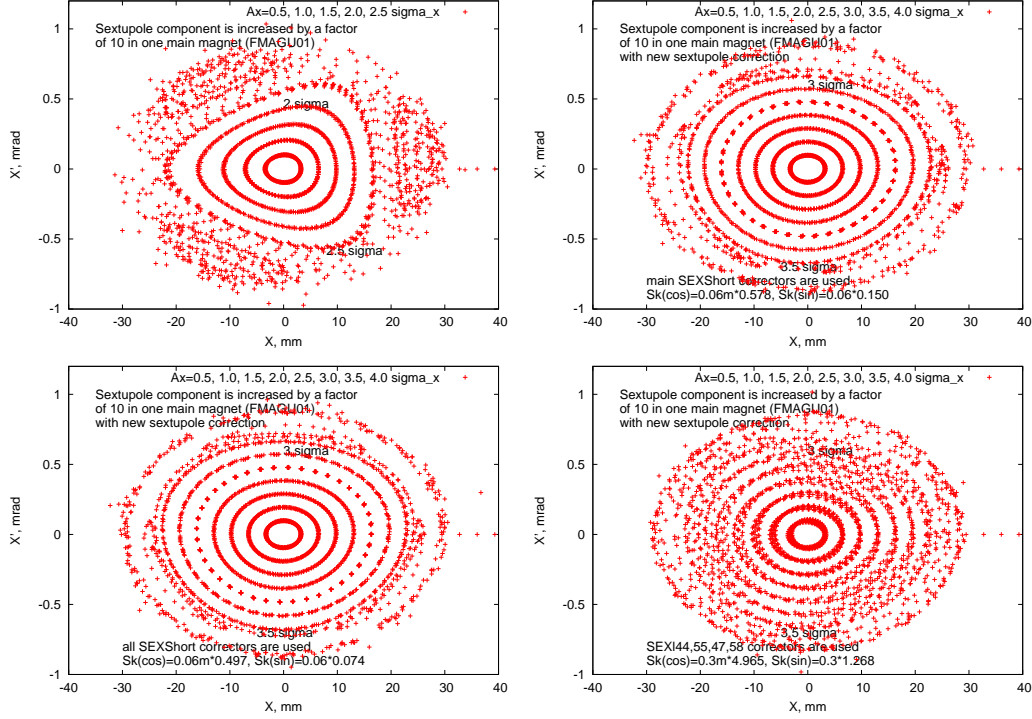


Figure 13: Horizontal phase plane of $A_x = 0.5 - 4.0\sigma_x$ particles ($\varepsilon_{95\%} = 7.8 \text{ mm} \cdot \text{mrad}$) for sextupole component increased by factor of 10 in focusing magnet FMAGU01 (top, left). Phase plane after correction using new main SEXS correctors with strength $Sk_{cos} = 0.06 \text{ m} \cdot 0.5776 \text{ m}^3$, $Sk_{sin} = 0.06 \text{ m} \cdot 0.1504 \text{ m}^3$ (top, right), using all new SEXS correctors with strength $Sk_{cos} = 0.06 \text{ m} \cdot 0.4970 \text{ m}^3$, $Sk_{sin} = 0.06 \text{ m} \cdot 0.0741 \text{ m}^3$ (bottom, left) and using old correction scheme with strength $Sk_{cos} = 0.3 \text{ m} \cdot 4.965 \text{ m}^3$ [SEXL55, SEXL47], $Sk_{sin} = 0.3 \text{ m} \cdot 1.265 \text{ m}^3$ (bottom, right) [SEXL44, SEXL58].